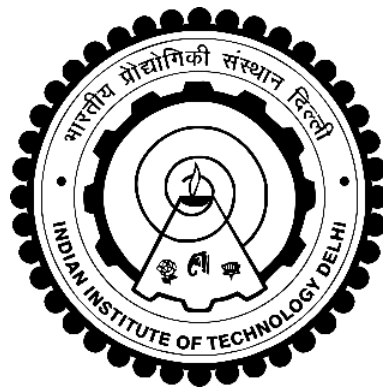


NANOTRIBOLOGY AND NANOMECHANICS OF HUMAN ARTICULAR CARTILAGE INTERFACES USING MOLECULAR DYNAMICS SIMULATIONS

ABHINAVA CHATTERJEE



**DEPARTMENT OF MECHANICAL ENGINEERING
INDIAN INSTITUTE OF TECHNOLOGY DELHI**

OCTOBER 2022

© **Indian Institute of Technology Delhi (IITD), New Delhi, 2022**

NANOTRIBOLOGY AND NANOMECHANICS OF HUMAN ARTICULAR CARTILAGE INTERFACES USING MOLECULAR DYNAMICS SIMULATIONS

by

ABHINAVA CHATTERJEE

Department of Mechanical Engineering

Submitted

in fulfillment of the requirements for the award of the degree of Doctor of Philosophy

to the



INDIAN INSTITUTE OF TECHNOLOGY DELHI

OCTOBER 2022

CERTIFICATE

This is to certify that the thesis entitled “**Nanotribology and Nanomechanics of Human Articular Cartilage Interfaces Using Molecular Dynamics Simulations**” is being submitted by **Mr. ABHINAVA CHATTERJEE** to the Indian Institute of Technology Delhi for the award of the degree of Doctor of Philosophy, is a record of original research work carried out by him using institute resources wherever required. **Mr. ABHINAVA CHATTERJEE** has worked under our guidance and supervision and has fulfilled the requirements for the submission of the doctoral thesis. The results and analysis contained in this thesis have not been submitted in part or in full to any other University or Institute for the award of any degree or diploma.

Prof. Devendra K. Dubey

(Supervisor)

Associate Professor

Department of Mechanical Engineering

Indian Institute of Technology Delhi

Prof. Sujeet K. Sinha

(Supervisor)

Professor

Department of Mechanical Engineering

Indian Institute of Technology Delhi

Date:

New Delhi

Acknowledgements

I would like to humbly acknowledge my advisors Prof. Devendra Kumar Dubey and Prof. Sujeet Kumar Sinha for their continuous support and motivation during my duration of doctoral studies at IIT Delhi. I am very grateful for being under the guidance of such kind, humble, creative personalities who always encouraged me in different unique ways during arduous situation during the research. I have learned a lot from their truthfulness and ethical attitude which I deeply understand are the core of quality research. I would also like to thank members of my dissertation committee, Prof. Satyendra Pal Singh, Prof. Raj Kumar Pandey, and Prof. Dinesh Kalyanasundaram for their valuable and critical comments which really helped me to improve the quality of work. I would like to thank Prof. Sangeeta Kohli, Prof. Jayashree Bijwe, and Prof. Sudarsan Ghosh and for their kind support during my difficult situations.

To achieve the final goal of doctoral thesis the pathways had many peaks and valleys, rather more valleys than peaks. These periods of downfall have not been bearable without the support of beloved friends and colleagues Dr. Mainendra Dewangan, Mr. Devershi Mourya, Dr. Siddharth Tamang, Mr. Jaswant K. Hirawani, Mr. Ashutosh Pandey, Dr. Surojit Poddar, Dr. Saurabh Chandrakar, Mr. Nikhil Sharma, Mr. Abhishek Singh, Dr. Girish C. Verma, Dr. Akhilesh Dadaniya, Dr. Amit Kumar, Dr. Ved Prakash, Dr. Rajesh Maddarkar, Dr. Ravi Kumar, Dr. Chiranjit Ray, Mrs. Mrinal Patel, Dr. Kanka Goswami, and Dr. Prithviraj Mukhopadhyay. Their constant support kept me moving on the right track. I would like to thanks to all the members and admin of CAGI Lab and MMC Lab for their good deeds, constant support and a healthy discourse.

Faculty members of IIT Delhi who have played a major role in my journey at IIT Delhi. I would like to thank specially Prof. Subir Kumar Saha (Ex-HOD Mechanical Engineering Department), Prof. Naresh Varma Datla, Prof. J.K. Dutt, Prof. S.S. Bahga, Prof. H. Hirani, Prof. M.R. Ravi (Current HOD), Prof. Debabrata Dasgupta, Prof. Subra Datta, and Prof. Pulak Mohan Pandey, Prof. S.K. Mohammed for their valuable suggestions. I would like to thank the efforts of staff of Department of Mechanical Engineering, Computer Service center for availing the facility of HPC which played a crucial role in my research.

I am very fortunate for being blessed with parents Mr. Samir Kumar Chatterjee and Mrs. Pranati Chatterjee who have always motivated me and encouraged for an affirmative action during tough times. I would like to remember and pay respect to by beloved brother and maternal grandfather whom I lost during this journey. Lastly, I would like to express my greatest gratitude to the God Almighty Lord Shiva and Lord Krishna for being a source of constant hope and energy to achieve new heights in personal and career development.

Abstract

Articular cartilage is a water-lubricated naturally occurring biological interface imparting unique mechanical and ultra-low frictional properties in mammalian bone joints. Nanoscale friction mechanism at the articular cartilage interface plays a significant role in the biomechanical functionality of the joints for millions of articulation cycles at several orders (obtained in-vitro 2 s^{-1} - $70 \mu\text{m s}^{-1}$) of shear rates providing low friction and wear properties. The superior lubricating properties ($\mu < 0.001$) at a contact pressure in the range of 1-6 MPa for the case of human hip and knee joints are attributed to the complex intermolecular interactions at the topmost superficial amorphous layer of several macromolecules/surfactants under confinement created by opposing cartilage surfaces experiencing various shear rates. Although the material of cartilage, synovial fluid composition, and their lubricating modes and properties have been extensively investigated at various length scales experimentally, there is still a lack of understanding of load-bearing, adhesion, and friction mechanisms of cartilage-cartilage interface from an atomistic perspective under heavy loading. This study is an attempt to systematically investigate the nanoscale mechanisms of contact, adhesion and boundary lubrication prevailing on the top surface of the human cartilage-cartilage interface in hip/knee joints and the influence of factors affecting the same using a molecular dynamics approach. Moreover, the effect of structural hierarchy aspects and chemical environment on the nanoscale friction is also investigated from a mechanistic approach. For this purpose, initially a proposed simplified atomistic model for a localized portion of top layer unhydrated cartilage-cartilage contact consisting of Collagen Type II representative units in the form of a slider and substrate is investigated for nanoscale adhesion and frictional properties. The frictional characteristics based on sliding tests in an unhydrated nanoscale environment are compared with existing nanotribological AFM experiments from literature.

Sliding tests show that friction is load and direction-dependent with an overall coefficient of friction (COF, μ) obtained in the range of 0.20 – 0.75 in comparison to $\mu=0.25$ obtained in experimental analysis for unhydrated fibrillar collagen contact interface. Pull-off tests of cartilage-cartilage contact interface reveal that cohesive interactions occur at the intercartilage interface due to formation of heavily interpenetrated atomistic sites leading to collagen stretching, extension, deformation and localized pulling of fragments during sliding. Analysis of interfacially hydrated intercartilage contact model reveals that interfacial water inhibits debonding at the interface during a pull-off test at higher loads. Interfacial debonding at the nanoscale is an important aspect of failure in heavily loaded asperity contact which occurs due to the rupture of H-bonds in the absence of water molecules. Thus, the study provides insights into the correlation of loading with the debonding characteristics. Sliding tests at higher load reveal water encapsulation by collagen side groups leading to significant reduction in the frictional forces up to five times in comparison to dry collagen-collagen contact. Sliding analysis performed on top layer fully tissue like hydrated cartilage-cartilage contact interface using varied loading and sliding velocity reveals that under maximum compression, and at lower speeds, pure dynamic sliding with enhanced interfacial water flow, adsorption, and mixing of water across interface lead to ultralow friction. An increase in sliding speeds at higher loads leads to interfacial water rearrangement, densification, and ordering inside confinement for resisting deformation imparting a uniquely low COF in the range of 0.01-0.09. An additional analysis of the local concentration of the ions present at the cartilage interface states a significant lowering in the mechanical and frictional behavior of the interface. It is observed that the nanofriction at the cartilage contact interface is dependent on the type, concentration and the combination of inorganic ions present at the interface. Current work contributes to the fundamental understanding of nanoscale interaction mechanics associated with

the contact, adhesion, and frictional behavior exhibited at the naturally occurring biological interfaces. Furthermore, this investigation reveals a nanomechanical understanding of the additional contribution of loading, interfacial hydration, various shear rates, local ionic environment, and concentration on the origins of ultralow friction at intercartilage lubricated interfaces. Present investigations contribute towards the design of tailored interactions in the development of alternative approaches in artificial implant research.

सार

आर्टिकुलर कार्टिलेज एक पानी-चिकनाई स्वाभाविक रूप से होने वाला जैविक इंटरफ़ेस है जो स्तनधारी हड्डी के जोड़ों में अद्वितीय यांत्रिक और अल्ट्रा-लो घर्षण गुण प्रदान करता है। आर्टिकुलर कार्टिलेज इंटरफ़ेस में नैनोस्केल घर्षण तंत्र कम घिसाव प्रदान करने वाले कतरनी दरों के कई आदेशों (इन-विट्रो 2 एस-1 -70 माइक्रोन एस -1 प्राप्त) पर लाखों आर्टिक्यूलेशन चक्रों के लिए जोड़ों की बायोमेकेनिकल कार्यक्षमता में महत्वपूर्ण भूमिका निभाता है। मानव कूल्हे और घुटने के जोड़ों के मामले में 1.9-6 एमपीए की सीमा में संपर्क दबाव पर बेहतर स्नेहन गुण ($\mu < 0.001$) को कई मैक्रोमोलेक्यूल्स/सर्फैक्टेंट्स की सबसे ऊपरी सतही अनाकार परत पर जटिल इंटरमॉलिक्युलर इंटरैक्शन के लिए जिम्मेदार ठहराया जाता है। विभिन्न कतरनी दरों का अनुभव करते हुए उपास्थि सतहों का विरोध करके बनाया गया कारावास। यद्यपि उपास्थि की सामग्री, श्लेष द्रव संरचना, और उनके स्नेहन मोड और गुणों की प्रयोगात्मक रूप से विभिन्न लंबाई के पैमानों पर बड़े पैमाने पर जांच की गई है, फिर भी कार्टिलेज-कार्टिलेज इंटरफ़ेस के लोड-बेयरिंग, आसंजन और घर्षण तंत्र की समझ की कमी है। भारी भार के तहत परमाणु परिप्रेक्ष्य। यह अध्ययन कूल्हे/घुटने के जोड़ों में स्तनधारी कार्टिलेज-कार्टिलेज इंटरफ़ेस की ऊपरी सतह पर मौजूद संपर्क, आसंजन और सीमा स्नेहन के नैनोस्केल तंत्र की व्यवस्थित रूप से जांच करने का एक प्रयास है और आणविक गतिकी दृष्टिकोण का उपयोग करके इसे प्रभावित करने वाले कारकों का प्रभाव है। इसके अलावा, नैनोस्केल घर्षण पर संरचनात्मक पदानुक्रम पहलुओं और रासायनिक वातावरण के प्रभाव की भी एक यंत्रवत दृष्टिकोण से जांच की जाती है। इस उद्देश्य के लिए, शुरू में एक स्लाइडर और सबस्ट्रेट के रूप में कोलेजन टाइप II प्रतिनिधि इकाइयों से युक्त शीर्ष परत निर्जलित उपास्थि-उपास्थि संपर्क के एक स्थानीय हिस्से के लिए एक प्रस्तावित सरलीकृत परमाणु मॉडल की जांच नैनोस्केल आसंजन और घर्षण गुणों के लिए की जाती है। एक निर्जलित नैनोस्केल वातावरण में स्लाइडिंग परीक्षणों पर आधारित घर्षण विशेषताओं की तुलना साहित्य से मौजूदा नैनोट्रिबोलॉजिकल एएफएम प्रयोगों से की जाती है। स्लाइडिंग परीक्षणों से पता चलता है कि घर्षण भार और दिशा-निर्भर है, जो घर्षण के समग्र गुणांक (COF, μ) के साथ 0.20 - 0.75 की सीमा में प्राप्त होता है, जबकि निर्जलित फाइब्रिलर कोलेजन संपर्क इंटरफ़ेस के लिए प्रयोगात्मक विश्लेषण में प्राप्त $\mu =$

0.25 की तुलना में। पुल-ऑफ परीक्षणों से पता चलता है कि इंटरकार्टिलेज इंटरफेस में भारी अंतःस्थापित परमाणु साइटों के गठन के कारण संयोजी अंतःक्रियाएं होती हैं जिससे कोलेजन खिंचाव, विस्तार, विरूपण और स्लाइडिंग के दौरान टुकड़ों के स्थानीयकृत खींचने की ओर अग्रसर होता है। इंटरफेशियली हाइड्रेटेड इंटरकार्टिलेज कॉन्टैक्ट मॉडल के विश्लेषण से पता चलता है कि उच्च भार पर पुल-ऑफ टेस्ट के दौरान इंटरफेसियल वॉटर इंटरफेस पर डिबॉन्डिंग को रोकता है। नैनोस्केल पर इंटरफेशियल डिबॉन्डिंग भारी भारित एस्पिरिटी संपर्क में विफलता का एक महत्वपूर्ण पहलू है जो पानी के अणुओं की अनुपस्थिति में एच-बॉन्ड के टूटने के कारण होता है। इस प्रकार, अध्ययन डिबॉन्डिंग विशेषताओं के साथ लोडिंग के सहसंबंध में अंतर्दृष्टि प्रदान करता है। उच्च भार पर स्लाइडिंग परीक्षणों से पता चलता है कि कोलेजन पक्ष समूहों द्वारा पानी के एनकैप्सुलेशन को शुष्क कोलेजन-कोलेजन संपर्क की तुलना में घर्षण बलों में पांच गुना तक महत्वपूर्ण कमी आई है। विभिन्न लोडिंग और स्लाइडिंग वेग का उपयोग करते हुए हाइड्रेटेड कार्टिलेज-कार्टिलेज कॉन्टैक्ट इंटरफेस जैसे पूरी तरह से ऊतक पर किए गए स्लाइडिंग विश्लेषण से पता चलता है कि अधिकतम संपीड़न के तहत, और कम गति पर, शुद्ध गतिशील स्लाइडिंग बढ़ाया इंटरफेसियल जल प्रवाह, सोखना, और इंटरफेस लीड में पानी का मिश्रण अल्ट्रा लो घर्षण के लिए। उच्च भार पर स्लाइडिंग गति में वृद्धि से 0.01-0.09 की सीमा में एक विशिष्ट रूप से कम COF प्रदान करने वाले विरूपण का विरोध करने के लिए अंतर्संबंधीय जल पुनर्व्यवस्था, घनत्व, और आंतरिक कारावास का आदेश दिया जाता है। उपास्थि इंटरफेस में मौजूद आयनों की स्थानीय एकाग्रता का एक अतिरिक्त विश्लेषण इंटरफेस के यांत्रिक और घर्षण व्यवहार में एक महत्वपूर्ण कमी बताता है। यह देखा गया है कि कार्टिलेज कॉन्टैक्ट इंटरफेस पर नैनोफ्रिक्शन इंटरफेस में मौजूद अकार्बनिक आयनों के प्रकार, एकाग्रता और संयोजन पर निर्भर है। वर्तमान कार्य स्वाभाविक रूप से होने वाले जैविक इंटरफेस में प्रदर्शित संपर्क, आसंजन और घर्षण व्यवहार से जुड़े नैनोस्केल इंटरैक्शन यांत्रिकी की मौलिक समझ में योगदान देता है। इसके अलावा, इस जांच से इंटरकार्टिलेज लुब्रिकेटेड इंटरफेस पर अल्ट्रा लो घर्षण की उत्पत्ति पर लोडिंग, इंटरफेसियल हाइड्रेशन, विभिन्न कतरनी दरों, स्थानीय आयनिक एकाग्रता के अतिरिक्त योगदान की एक नैनोमैकेनिकल समझ का पता चलता है। वर्तमान जांच कृत्रिम प्रत्यारोपण अनुसंधान में वैकल्पिक दृष्टिकोण के विकास में अनुरूप बातचीत के डिजाइन की दिशा में योगदान करती है।

Table of Contents

| | | |
|--------------------|--|-----------|
| CHAPTER - 1 | INTRODUCTION | 1 |
| 1.1 | MECHANICS AND TRIBOLOGY OF HUMAN JOINTS | 1 |
| 1.1.1 | <i>Tribology</i> | 3 |
| 1.2 | TRIBOLOGY OF ARTICULAR CARTILAGE | 5 |
| 1.3 | IMPLANTS | 8 |
| 1.4 | NANOSCALE FRICTION, LUBRICATION, AND ITS SIGNIFICANCE | 11 |
| 1.5 | NANOMECHANICAL STUDY OF CARTILAGE TOP LAYER | 13 |
| 1.6 | OUTLINE OF THESIS | 14 |
| CHAPTER - 2 | REVIEW OF LITERATURE | 19 |
| 2.1 | NATURAL LUBRICATION ON CARTILAGE AND REGIMES | 20 |
| 2.2 | BOUNDARY LUBRICATION AT THE CARTILAGE INTERFACE | 24 |
| 2.3 | CARTILAGE TOP LAYER COMPOSITION STRUCTURE, CONSTITUENTS, FUNCTIONS, AND NANOSCALE INTERACTIONS | 28 |
| 2.4 | MOLECULAR MECHANISM OF BOUNDARY LUBRICATION STUDIES AT THE TOP LAYER CARTILAGE INTERFACE | 31 |
| 2.5 | MOLECULAR DYNAMICS SIMULATIONS OF INTERFACIAL INTERACTIONS | 33 |
| 2.6 | POTENTIAL GAPS IN THE NANOSCALE FRICTION UNDERSTANDING AT CARTILAGE | 38 |
| 2.7 | OBJECTIVE OF THESIS | 39 |
| CHAPTER - 3 | MOLECULAR SIMULATIONS FRAMEWORK AND METHODOLOGY | 47 |
| 3.1 | MOLECULAR DYNAMICS METHODOLOGY | 51 |
| 3.2 | DEVELOPMENT OF REPRESENTATIVE ATOMISTIC MODEL OF TOP LAYER CARTILAGE LOCALIZED CONTACT | 51 |
| 3.3 | MOLECULAR SIMULATION SETUP AND SIMULATION FRAMEWORK | 57 |
| 3.3.1 | <i>Pull-off Test</i> | 60 |
| 3.3.2 | <i>Sliding Test</i> | 62 |

| | | |
|-----|--------------------------------------|----|
| 3.4 | INITIAL RESULTS AND VALIDATION | 66 |
|-----|--------------------------------------|----|

CHAPTER - 4 EFFECT OF LOADING ON THE NANOSCALE ADHESION AND FRICTION AT THE UNHYDRATED CARTILAGE-CARTILAGE TOP LAYER

INTERFACE 72

| | | |
|-----|--|----|
| 4.1 | INTRODUCTION | 72 |
| 4.2 | METHODOLOGY AND FRAMEWORK | 73 |
| 4.3 | RESULTS AND DISCUSSION | 73 |
| | 4.3.1 <i>Nanoscale Adhesive behavior of unhydrated cartilage interface</i> | 74 |
| | 4.3.2 <i>Nanoscale Frictional behavior of unhydrated articular cartilage</i> | 81 |
| | 4.3.3 <i>Effect of load on the Average Friction Coefficient (COF)</i> | 89 |
| 4.4 | CHAPTER SUMMARY AND INSIGHTS | 93 |

CHAPTER - 5 EFFECT OF LOADING ON THE NANOSCALE FRICTION AND ADHESION MECHANISMS AT ARTICULAR CARTILAGE TOP LAYER

HYDRATED INTERFACES 96

| | | |
|-----|---|-----|
| 5.1 | INTRODUCTION | 96 |
| 5.2 | METHODOLOGY..... | 101 |
| | 5.2.1 <i>Interface hydrated contact model</i> | 101 |
| | 5.2.2 <i>Simulation Setup</i> | 103 |
| 5.3 | RESULTS AND DISCUSSIONS | 107 |
| | 5.3.1 <i>Effect of loading on the load-bearing capacity and water diffusion</i> | 108 |
| | 5.3.2 <i>Effect of loading on the pull-off characteristics</i> | 110 |
| | 5.3.3 <i>Frictional behavior under external loading</i> | 115 |
| 5.4 | CHAPTER SUMMARY AND INSIGHTS | 124 |

CHAPTER - 6 EFFECT OF SLIDING VELOCITY ON THE NANOSCALE FRICTION BEHAVIOR OF ARTICULAR CARTILAGE CONTACT INTERFACE

| | | |
|-----|---|-----|
| 6.1 | INTRODUCTION..... | 127 |
| 6.2 | METHODOLOGY..... | 131 |
| | 6.2.1 <i>Development of Atomistic model of fully hydrated cartilage-cartilage contact</i> | 131 |
| | 6.2.2 <i>Simulation Methodology.....</i> | 133 |
| 6.3 | RESULTS AND DISCUSSIONS | 135 |
| | 6.3.1 <i>Effect of sliding speed on the Frictional behavior.....</i> | 136 |
| | 6.3.2 <i>Directional dependency of friction.....</i> | 147 |
| | 6.3.3 <i>Effect of sliding velocity on the Friction Coefficient</i> | 153 |
| | 6.3.4 <i>Effect of sliding velocity on the interface temperature</i> | 155 |
| 6.4 | CHAPTER SUMMARY AND INSIGHTS | 157 |

CHAPTER - 7 NANOSCALE FRICTION MECHANISMS ON ARTICULAR

CARTILAGE INTERFACE IN DIFFERENT IONIC ENVIRONMENTS 163

| | | |
|-----|---|-----|
| 7.1 | INTRODUCTION..... | 163 |
| 7.2 | METHODOLOGY..... | 165 |
| 7.3 | RESULTS AND DISCUSSIONS | 166 |
| | 7.3.1 <i>Effect of type of ions on nanoscale frictional behavior</i> | 166 |
| | 7.3.2 <i>Effect of ionic concentration on the nanoscale friction properties at cartilage interface</i> | 175 |
| | 7.3.3 <i>Effect of combination of ions on the frictional properties</i> | 182 |
| | 7.3.4 <i>Effect of velocity on the combined cartilage model.....</i> | 184 |
| 7.4 | CHAPTER SUMMARY AND INSIGHTS | 187 |

CHAPTER - 8 CONCLUSIONS AND FUTURE DIRECTIONS 189

LIST OF FIGURES

Figure 1.1 Schematic representation of the Hip joint a) Human hip joint, b) Articular cartilage, c) Composition of the cartilage matrix. Image adapted from (Gottardi et al., 2016), d) cartilage on cartilage contact, e) Anatomy of top layer cartilage. 3

Figure 2.1 Flowchart of human hip joint lubrication 23

Figure 2.2 Articular Cartilage-cartilage contact at various scales. 25

Figure 2.3 Stribeck curves for lubrication regimes of a sliding process in comparison to that of natural lubrication [Graph redrawn from ref. (Daniel, 2014)]. 27

Figure 2.4 Flowchart of investigating the nanoscale friction phenomenon at the articular cartilage. 40

Figure 3.1 Hierarchical Structure of top layer cartilage-cartilage contact interface with the proposed three-dimensional atomistic model for MD simulations. (a) Schematic of top layer cartilage-cartilage contact at the knee joint, (b) Topmost layer of the SAL in Extracellular Matrix (ECM) made up of collagen fibres arranged tangentially to the sliding direction, (c) SEM Image of collagen fiber at the knee. Image obtained under the terms of the Creative Commons Attribution License, (d) Schematic of Prototypic fiber which makes up the collagen fiber, (e) Representation of collagen heterofibril, (f) Atomistic model of cartilage in form of a slider using a representative fragment, (g) collagen type II fragment chosen for the study and (h) The atomistic representation of the portion highlighted where Oxygen, Nitrogen, Sulphur, Carbon and hydrogen are represented in red, blue, yellow, gray and white spheres. 53

Figure 3.2 Three-dimensional proposed atomistic model of a top layer cartilage-cartilage unhydrated contact. (a) A single representative fragment is chosen for the development of a model consisting of three identical helical chains of amino acid sequence (GPMGPMGPRGPP). A single green chain has been demarked with its amino acid constituents (Glycine, Proline and Methionine) of which atomic structure of Glycine is explicitly shown, (b) Isometric view of the proposed atomistic model in form of slider and substrate depicting only two fragments both in its atomistic and helical representation. Each cylinder represents a single collagen fragment, (c) Front view of the proposed atomistic model of top layer cartilage-cartilage unhydrated contact with collagen fragment arranged into the plane along its axis and (d) Right-hand side view of the proposed atomistic model. Rendered using VMD(Humphrey, W.; Dalke, A.; Schulten, 1996). 56

Figure 3.3 (a) Schematic Representation of simulation methodology for the pull-off test of top layer cartilage-cartilage interface atomistic model. The top block is being pulled whereas the dynamics is studied on the deformable atoms both at the top intra-cartilage interface and the inter-

cartilage interface, (b) Three-dimensional representation of different layers considered and their role in obtaining the normal and frictional force for both pull-off and friction tests. Force is calculated on all the green atoms due to all the pink atoms to obtain the normal and frictional force at the interface. The orange layer represents the thermostatted layer where the temperature is scaled as the sliding takes place. 61

Figure 3.4 Schematic and three-dimensional model for conducting non-equilibrium molecular dynamics (a) Representation of the friction simulation methodology as normal force is applied on the topmost layer with the middle layer kept at a constant temperature using a thermostat and interfacial forces are being obtained on the bottommost layer of the slider, (b) Schematic for conducting friction simulations perpendicular along X-axis and parallel along Z axis. Upper Slider block marked in dotted blue is slid against the lower substrate both parallel and perpendicular to the collagen axes, (c) Simulation methodology and distribution of layer for conducting friction simulations in the form of a slider and substrate in the atomistic model as the representation shown in Figure 4(a). Each of the circles represents a collagen fragment chosen. The normal and shear forces are computed as the summation of forces obtained at each time step along y and x-direction on the top Newtonian atoms of the slider due to the Newtonian atoms of the substrate. Frictional forces are resolved opposite to the motion and equal in the magnitude of shear forces obtained. The Newtonian atoms of the slider are represented in green and that of the substrate in pink as shown in the force methodology depicted in Figure 3(b). 65

Figure 4.1 (a) Variation curve of normal force obtained at the inter-cartilage interface vs distance of separation of the top block. The Topmost layer is pulled as shown in the schematic and force is measured on the blue atoms due to the red atoms to predict the adhesive behavior of the inter-cartilage, (b) Variation of total interaction energy with the distance of separation at the top layer inter-cartilage interface. Higher load leads to higher attraction due to a decrease in energy indicative of cohesive interactions and increased pull, (c) Pull-off test trajectory visualization for various loads during pull-off test. Amino acid shown in yellow (MET) of the slider is entangled deeply into the substrate and act as cohesive sites for localized pull at higher loads L28 case. .. 77

Figure 4.2 Variation curve of normal force obtained at the intra-cartilage interface vs distance of separation of the top block, (b) Variation of total interaction energy at the top slider bed surface atoms due to the substrate atoms. Increase in load leads to heavy atomistic locking and longer stretching length of collagen fragments, (c) Pull-off test trajectory at various stages of the adhesion test. High cohesion at the inter-cartilage interface leads to detachment of the topmost layer at the intra-cartilage interface. Rendered using VMD(Humphrey, W.; Dalke, A.; Schulten, 1996)..... 79

Figure 4.3 Nanoscale Friction force variation with time in picoseconds (ps) at the top layer inter-cartilage interface while sliding perpendicular to the collagen axis, (b) Normal force variation with time for perpendicular sliding, (c) Nanoscale Friction force variation against time while sliding parallel to the collagen axis and (d) Normal force variation with time for parallel sliding. Three zones of frictional process static zone, geometry dependent and deformation zone shown in blue, golden and white color. Average friction coefficient (COF) calculated in golden colored zone. 83

Figure 4.4(a) Schematic representing geometry dependent movement and friction in perpendicular sliding. Blue arrow represents the direction of the motion of the upper slider collagen layer on the substrate collagen layer, (b) geometry dependent movement and friction in parallel sliding, (c) Stages of sliding of top layer cartilage-cartilage unhydrated atomistic model perpendicular to the collagen axes indicating the three zones of friction process .i.e. initial zone, geometry dependent zone and deformation zone. The red dotted box shows the movement of the topmost layer in x-direction and the bottommost red dotted box shows the fixed region of the substrate for frictional simulations and (d) Stages of sliding of unhydrated atomistic model parallel to the collagen axes. All the collagen fragments are shown in tube representation of VMD and the blue and red tubes represents the topmost portions of the slider and the substrate, other portions are marked in gray color(Humphrey, W.; Dalke, A.; Schulten, 1996). 87

Figure 4.5 (a) Type of interaction at the inter-cartilage interface. The blue atoms are the atoms of the bottommost layer of the top slider which is under pull and red atoms of the lower substrate. Load bearing happens at such discrete sites which consist of Type A, B, C interactions respectively, (b) Snapshots of the inter-cartilage interface during the friction phenomenon sliding perpendicular. At higher load the cohesive sites represented in blue are stretched and offer localized pull to resist the deformation due to sliding. Rendered using VMD(Humphrey, W.; Dalke, A.; Schulten, 1996). 88

Figure 4.6 Interlayer sliding and initiation of sliding with load (a) Interlayer sliding deformation in sliding parallel (b) Variation of interlayer sliding initiation with load. At higher load this deformation is earlier. 89

Figure 4.7 Comparison of average friction coefficient (COF) obtained in parallel and perpendicular sliding (a) Variation of COF with load and sliding orientation. COF higher in parallel case due to constant number of H-bonds at the interface and (b) Number of H bonds with respect to Sliding distance (for $d=1 \text{ \AA}$, time $t=100 \text{ ps}$). At $d=7 \text{ \AA}$ the number of H-bonds dips and interlayer sliding initiates. 90

Figure 4.8 Comparison of scale and localized contact mechanism. The red and the black circles denote the asperity-asperity contact at the top layer. Magnified view of the area of interest presents a difference in scale of the surface and the MD model developed in the present study. 93

Figure 5.1 Structural hierarchy of the articular cartilage and developed cartilage interfacial hydrated model (a) Schematic representation of cartilage-cartilage synovial fluid lubricated contact at human hip joint, (b) cross-sectional representation of top layer cartilage hydrated contact within sandwiched collagen layer, (c) transverse section of a single layer of the microscale top layer consisting of collagen fibrils, (d) proteolytic collagen fiber present tangentially at the surface, (e) representation of collagen heterofibril, contact between two heterofibril at the cartilage, (f) cartilage-cartilage interfacial contact in form of a collagen-collagen heterofibril contact (g)atomistic cartilage-cartilage interface hydrated model in form of a slider and substrate made up of collagen fragments marked in yellow cylinders with confined water in between, (h) collagen type II fragment used for the study (i) molecular portion of the collagen fragment with atomistic

representation with carbon, hydrogen, Sulphur, nitrogen, oxygen shown in gray, white, yellow, blue and red respectively. 99

Figure 5.2 Atomistic model of cartilage-cartilage top layer interfacial hydrated contact model (a) Collagen fragment in the form of triple helix used for constructing the atomistic model. One of the chains is shown with few of its amino acid residues. The atomistic structure of Glycine is shown, (b) the front view of the cartilage-cartilage top layer interface hydrated contact model. Each circle denotes a collagen fragment placed inward to the plane in z-direction and (c) Side view of the atomistic model. Collagen fragments are shown in tube representation of VMD(Humphrey, W.; Dalke, A.; Schulten, 1996). 103

Figure 5.3 Schematic representation of non-equilibrium molecular dynamics (a) simulation methodology for pull-off and sliding test on the cartilage-cartilage top layer interface hydrated model (b) three-dimensional cartilage interface hydrated contact model represented in VDW representation of VMD with frictional simulation methodology. Rendered using VMD (Humphrey, W.; Dalke, A.; Schulten, 1996). The topmost layer is pulled for conducting a pull-off test and applied with a velocity for obtaining a frictional response. The interim layer above the deformable layers denoted in orange are thermostatted and force calculation performed on the deformable layer. 105

Figure 5.4 Loading characteristics of the cartilage-cartilage top layer interface hydrated model (a) Variation of total normal force against post-equilibration time at the top collagen-water interface (b) normal load variation of collagen-on-collagen underneath the confined water layer versus post-equilibration time (c) Snapshot of the atomistic model of the interface after minimization (d) Snapshot of compressed cartilage interface hydrated contact model at load=28 nN where collagen fragments are shown in ribbons representation and the water-seepage sites are marked in yellow color. 109

Figure 5.5 Pull-off characteristics of cartilage-cartilage top layer interfacial hydrated contact model (a) variation of total normal load at the top collagen-water interface with the separation distance (b) normal force of collagen-collagen at the interface with separation distance(c) total interaction energy variation with separation distance to study collagen-water intermolecular interactions and (d) interaction energy of collagen-collagen interaction versus separation distance through the water film. 113

Figure 5.6 Pull-off test trajectories of cartilage-cartilage top layer interfacial hydrated model. (a)Initialization of pull-off test, (b) load-bearing phenomenon at the interface, (c) localized stretching and breakage of H-bonds, and (d) debonding occurring at the cartilage interface shown in yellow dotted lines. Upward pull-off in the topmost layer enhances water molecules to percolate in the interfacial contact bearing load locally, preventing stretching by accumulating where collagen is in the vicinity. 113

Figure 5.7 Analysis of number of H-bond breakage at the cartilage interface (a) variation of number of H-bond at the collagen-water interface with the separation distance, (b) variation of number of

H-bond between water-water against separation distance at various loads, (c) snapshot of previously conducted dry collagen-collagen pull-off test denoting high cohesion at the interface due to formation of strong collagen-collagen H-bonds(Chatterjee, Dubey and Sinha, 2020). Separate image used and (d) Comparison of Number of H-bonds remaining at the interface with respect to the separation distance from previously conducted MD Simulations. 114

Figure 5.8 Frictional behavior of cartilage-cartilage top layer interfacial hydrated contact model (a) variation of frictional force with sliding distance at the cartilage interface while movement in z-direction parallel to the arrangement of collagen, (b) variation of frictional force at the cartilage interface in the direction perpendicular to the collagen axis, (c) total interaction energy obtained at the collagen-water interface against sliding distance in parallel direction movement, (d) total interaction energy at the collagen-water interface versus sliding distance in perpendicular direction movement and (e) comparison of frictional force during shearing of dry cartilage-cartilage interface with frictional force obtained at the collagen-water and collagen-collagen during sliding the interfacial hydrated model in a perpendicular direction at $L=28\text{nN}$ 119

Figure 5.9 Sliding dynamics trajectories of the cartilage-cartilage top layer interfacial hydrated model while sliding in the direction parallel (z-axis) to the collagen axis at two different loads $L=7\text{ nN}$ and $L=28\text{ nN}$. The interfacial layer comprises of the blue, red, and the water layer and shown in the ribbon representation of VMD(Humphrey, W.; Dalke, A.; Schulten, 1996), and sliding is performed in the negative Z-axis which is parallel to the collagen axis. 121

Figure 5.10 Snapshots of dynamic trajectories at various steps during sliding of the interface model in x-direction perpendicular to the collagen axis at two different loads $L=3.5\text{ nN}$ and $L=28\text{ nN}$. All the collagen fragments are denoted in ribbons representation and the Blue and red layer demarks the topmost layer closer to the interface having a water layer in between. Based on the load applied the number of water molecules at the interface fluctuates. At lower load, the attractive interaction of the collagen-water at the top interface pulls the substrate layer to engulf more water molecules. At higher load, the contact zones behave like a nanochannel carrying water molecules catering to lower shear forces at localized sites. 122

Figure 5.11 H-bond analysis for sliding of cartilage-cartilage top interfacial model (a) variation of h-bonds in water-water interactions with sliding distance in direction parallel to the collagen axis, (b) variation of h-bonds in water-water interactions with sliding distance in the perpendicular direction, (c) number of H-bonds against sliding distance for collagen-water interactions at the top interface in parallel direction movement and (d) number of H-bonds versus sliding distance for collagen-water interactions at the top interface in the direction perpendicular to collagen axis. 123

Figure 6.1 Articular Cartilage hierarchical structure and developed representative top layer cartilage-cartilage contact fully hydrated atomistic model. (a) Schematic of cartilage-cartilage topmost layer contact with synovial fluid within tangentially arranged collagen fibers. (b) A represented portion of the collagen-collagen fiber contact at the interface encapsulated in water. (c) Collagen heterofibrils consisting of collagen type II molecules at the periphery in contact with another heterofibril of opposite cartilage interface. (d) Developed top layer three-dimensional fully

hydrated articular cartilage-cartilage atomistic contact in front view (e) Isometric view of the atomistic model in a slider-substrate configuration in tube representation of VMD(Humphrey, W.; Dalke, A.; Schulten, 1996) showing a repeating collagen type II fragment in ribbon form. The collagen fragment shown inside the transparent cylinder is arranged tangentially in the -ve z-direction. (f) Collagen type II fragment chosen represented in three amino acid chains shown in red, blue, and green. Each of these colored chains is identical and has an amino acid sequence (GPMGPMGPRGPP)(Chatterjee, Dubey and Sinha, 2020, 2021). Color coding of the Elements present in the aminoacids of these collagen fragments is represented..... 129

Figure 6.2 Atomistic three-dimensional model to illustrate the nonequilibrium molecular dynamics methodology for conducting frictional simulations. The bottommost layer is fixed and the topmost layer is applied with a uniform load. Thereafter sliding test is performed in +ve X and -ve Z axis respectively by moving the topmost layer with three different orders of velocity. Normal and Frictional Forces are computed on the blue layer (Collagen-water interface) due to the nanoconfined water layer as shown in magnified view. The portion represented in green dotted lines is treated as the atomistic interface and the interfacial interaction energy and temperature are calculated in this region All the repeating collagen fragment units are shown in the new ribbon representation of VMD (Humphrey, W.; Dalke, A.; Schulten, 1996). 135

Figure 6.3 Sliding trajectories of top layer fully hydrated cartilage-cartilage contact at low loads for the three sliding velocities v1, v2, and v3. The perpendicular sliding collagens are in tube representation of VMD. Lower velocities show pure dynamic sliding at the collagen-water interface whereas higher velocity sliding is accompanied by subsurface deformation, collagen stretching, uncoiling, and intracartilage separation by sliding. In parallel sliding a small portion (water molecules within z=12 to z=15) has been highlighted to understand the behavior of the water molecules at the intra- and the intercartilage interface while sliding at three different velocities. Water inflow as an effect of Intracartilage separation. Rendered using VMD (Humphrey, W.; Dalke, A.; Schulten, 1996). 137

Figure 6.4 Obtained Normal Force and frictional force characteristics at the top layer fully hydrated articular cartilage-cartilage atomistic contact interface while sliding in the perpendicular direction as a function of varied load and sliding speed at top collagen-water interface. Characteristics for v1, v2, and v3 i.e. (0.01, 0.1, and 1 Å/ps) have been represented in red, blue, and green curves respectively for all the load cases. 139

Figure 6.5 Variation of Interaction energy at the top collagen-water interface with respect to sliding distance as a function of several loads and a range of velocities. Intercartilage interaction energy for all the cases is attractive. All the lowest velocity cases v1 possess the highest interaction energy as shown in red curves due to the maximum time of interaction at the interface. 144

Figure 6.6 Dynamic trajectories of sliding mechanism for L38v3x case at a localized zone where a side chain of collagen fragment is protruding as represented in blue color. The bottom collagen surface is denoted in red color. Water within 2-4Å of the top or bottom protein surface can bear the proportion of the load due to strong hydration forces. The upper collagen top surface is

represented in blue and red denotes collagen substrate. The water molecules within 3 Å of top surfaces are represented in red and the lower ones in gray. Visual and quantification show only a water molecule can pass through that molecular gap of 3.8Å. Rendered using VMD(Humphrey, W.; Dalke, A.; Schulten, 1996)..... 145

Figure 6.7 Comparison of the sliding dynamics of cartilage-cartilage atomistic contact at lowest velocity and the highest velocity cases. For all the low-velocity sliding cases pure dynamic sliding has been observed at the collagen-water interface. High-velocity sliding cases are accompanied by less relative interfacial movement at the collagen-water interface and subsurface deformations. For all the cases the bottom layer is fixed. All the collagen fragments are represented in the tube representation of VMD(Humphrey, W.; Dalke, A.; Schulten, 1996). Blue dotted lines represent the top moving layer whereas the black dotted lines represent visual subsurface deformation. L38v3x case has less deformation with more interfacial sliding..... 146

Figure 6.8 Interfacial water flow behavior captured at highest loads L38 for all the velocity cases. Maximum water movement was observed at v1 due to maximum interaction time for the realization of forces from the sliding top layer to the collagen-water interface. With an increase in velocity, at v3 water starts to densify, align, orient in the direction to bear the maximum normal load and shear deformation. Rendered using VMD(Humphrey, W.; Dalke, A.; Schulten, 1996). 147

Figure 6.9 Parallel Sliding Dynamic trajectories at the top layer cartilage-cartilage contact at maximum load L=38nN. A blue portion (z=12 to z=15Å) is denoted to show the subsurface shear deformation (δ) as the upper collagen slider moves. Rendered using VMD(Humphrey, W.; Dalke, A.; Schulten, 1996). 150

Figure 6.10 Obtained normal and friction force behavior at the articular cartilage-cartilage hydrated contact interface while moving in the parallel direction (-ve Z-axis) as a function of varied load and sliding speed. 152

Figure 6.11 Interfacial layer sliding behavior under different loading and sliding conditions. Blue and red tube structures denote the outermost layer of the top and bottom cartilage-contact interface across the confined water. Water molecules near to 3 Å of both the collagen surfaces are denoted in red and gray for top and bottom layers respectively. Rendered using tube representation in VMD for collagen fragments, CPK for surface waters, and line to represent bulk water (Humphrey, W.; Dalke, A.; Schulten, 1996)..... 152

Figure 6.12 Variation of Coefficient of Friction at the Collagen-water contact interface with respect to an increase in sliding velocity for both perpendicular and parallel sliding. The frictional behavior for loads L=9 nN, 19nN, and 38 nN are represented in black, red, and blue respectively. With an increase in the load, the change in the coefficient of friction is very less..... 154

Figure 6.13 Variation of obtained interface temperature (T_i) at the top layer collagen-water interface with load and increasing sliding speed. The increase in sliding velocity has a significant impact on the interface temperature rise. 157

Figure 7.1 Schematic details of the simulated ionic environments for conducting nanoscale sliding test at the cartilage interface. 168

Figure 7.2 Snapshots of the fully hydrated cartilage models in different ionic environments. The Calcium, Sodium, Potassium are represented in cyan, red, green colors respectively. Chloride ions are represented in black except the (e) where it is represented in blue color. (a) neutralized by adding Chloride ions in hydrated cartilage model (b) calcium incorporated Cartilage model (c) Sodium included cartilage model (d) Potassium in cartilage model (e) cartilage with only chloride ions (f) Purely hydrated cartilage model with no mobile charged ions. 168

Figure 7.3 Variation of frictional properties at the hydrated cartilage interface with sliding distance at different ionic environment containing different ions while sliding in direction (+ve X axis) perpendicular to the axis of the collagen fragments (a) Obtained normal force at the top collagen-water intercartilage interface for six ionic conditions i.e. calcium, sodium, potassium, chloride, neutral, and purely hydrated. All the cartilage models have Chloride added to them for counterbalancing. Calcium, Sodium, Potassium, Chloride, neutral, and purely hydrated are shown in Cyan, red, green, blue, black, and gray colors accordingly. Most of the ions are present at the cartilage interface, (b) Friction force curves for the six ionic environment (c) Non-bonded interaction energy at the cartilage interface for various ionic environment. 171

Figure 7.4 Loading and sliding trajectories of cartilage models added with Ca^{2+} and Cl^- in separate models. 171

Figure 7.5 Number of water molecules at the collagen-water interface. 172

Figure 7.6 Variation of nanoscale surface properties at the cartilage interface while sliding is performed in the direction (-ve Z axis) parallel to the collagen axis (a) Obtained normal force at the cartilage interface while sliding (b) Friction force at the sliding interface (c) interaction energy due to non-bonded forces at the collagen-water interface. 174

Figure 7.7 Dynamic Trajectories for sliding of cartilage interface at two different calcium concentrations in dissociated form. Heavy deformation has been observed at high ionic concentrations due to interplay of water with the protein residues. There is no observable deformation found in C_1 , C_2 , C_3 and C_4 176

Figure 7.8 Dynamic Trajectories for sliding of cartilage interface at two different sodium concentrations in dissociated form. Compressive deformation has been observed in almost all the models of cartilage tissue due to interplay of water at the surfaces. 177

Figure 7.9 Variation of interfacial properties with respect to sliding distance at the cartilage under different ionic concentrations (a) Obtained normal force for five different concentration levels of calcium in hydrated cartilage model. The concentrations C_1 , C_2 , C_3 , C_4 , and C_5 are denoted in red, blue, green, cyan and black respectively, (b)frictional force obtained at the cartilage interface while sliding, (c)Non-bonded interaction energy at the interface for the different calcium concentrations (d)normal force at different concentrations of Sodium in hydrated cartilage models (e)frictional force at the cartilage interface (f)interaction energy at the interface including the non-bonded interaction terms..... 179

Figure 7.10 Analysis of water molecules near to cartilage collagen-water interface. 182

Figure 7.11 Frictional behavior at the cartilage interface under different ionic environments. . 183

Figure 7.12 Sliding trajectories of CaNaK cartilage interface while sliding in the x-direction at varied sliding speeds. 186

Figure 7.13 Frictional properties of CaNaK hydrated cartilage model with respect to sliding distance. 186

LIST OF TABLES

| | |
|--|-----|
| Table 1.1 Mechanical properties of implant materials (Mattei et al., 2011)..... | 10 |
| Table 2.1 Lubricating mechanisms in natural joints [Table Ref: Peterson, Bronzino, Biomechanics-Principle and Application Table 4.1, Page 4-09]..... | 21 |
| Table 4.1 Dependence of Pull-off forces on the load applied. | 80 |
| Table 4.2 Comparison of COF obtained in perpendicular as well as the parallel movement of the slider..... | 91 |
| Table 6.1 Comparison of current MD cartilage friction study with previous studies | 154 |
| Table 7.1 Average Coefficient of Friction at the cartilage interface under different ionic conditions..... | 173 |
| Table 7.2 Coefficient of Friction of Calcium cartilage models at different concentrations. | 179 |
| Table 7.3 Coefficient of Friction for Sodium cartilage interface models under five different concentrations. | 181 |
| Table 7.4 Coefficient of friction for different cartilage models added in a combination of inorganic ions..... | 184 |
| Table 7.5 Frictional properties of CaNaK cartilage interface under varied sliding velocities. .. | 186 |